# Investigations of the Effect of the Non-Manganese Metal in Heterometallic-Oxido Cluster Models of the Oxygen Evolving Complex of Photosystem II: Lanthanides as Substitutes for Calcium

Po-Heng Lin, Michael K. Takase, and Theodor Agapie*

Division of Chemistry and Chemical Engineering, California Institute of Technology, Pasadena, California 91125, United States

Ⓢ *Supporting Information*

ABSTRACT: We report the syntheses and electrochemical properties of nine new clusters ($[LLnMn^{IV}_3O_4(OAc)_3(DMF)_n]^+$ (Ln = La^{3+}, Ce^{3+}, Nd^{3+}, Eu^{3+}, Gd^{3+}, Tb^{3+}, Dy^{3+}, Yb^{3+}, and Lu^{3+}, n = 2 or 3)) supported by a ligand (L^{3-}) based on a 1,3,5-triarylbenzene motif appended with alkoxide and pyridine donors. All complexes were obtained by metal substitution of Ca^{2+} with lanthanides upon treatment of previously reported $LMn_3CaO_4(OAc)_3(THF)$ with Ln(OTf)$_3$. Structural characterization confirmed that the clusters contain the $[LnMn_3O_4]$ cubane motif. The effect of the redox-inactive centers on the electronic properties of the Mn$_3$O$_4$ cores was investigated by cyclic voltammetry. A linear correlation between the redox

Biological OEC   Synthetic models

potential of the cluster and the ionic radii or pKa of the lanthanide metal ion was observed. Chemical reduction of the $LMn^{IV}_3GdO_4(OAc)_3(DMF)_2$ cluster with decamethylferrocene, resulted in the formation of $LGdMn^{IV}_2Mn^{III}O_4(OAc)_3(DMF)_2$, a rare example of mixed-valence $[MMn_3O_4]$ cubane. The lanthanide-coordinated ligands can be substituted with other donors, including water, the biological substrate.
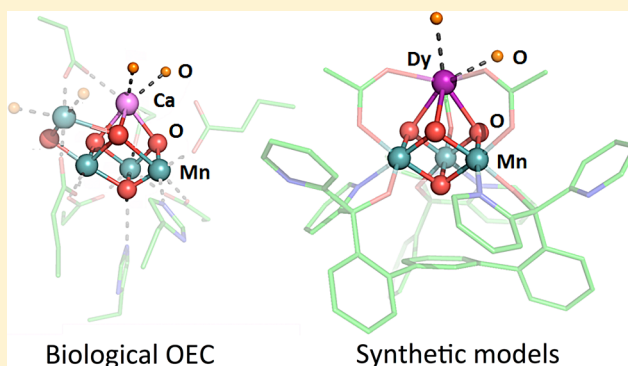
Biological water oxidation occurs in photosystem II (PSII) at the oxygen-evolving complex (OEC), an inorganic cluster displaying a Mn$_4$CaO$_n$ moiety.[1] Single crystal X-ray diffraction (XRD) studies have revealed that the OEC consists of a distorted Mn$_3$CaO$_4$ cubane bridged to the fourth Mn via oxide moieties.[2] During catalysis, the OEC undergoes four electron transfer events, leading to a high oxidation state Mn cluster capable of promoting O—O bond formation and release of O$_2$.[3] Although its role remains under debate, the Ca^{2+} ion is instrumental for catalysis.[4] Ca^{2+} has been proposed to affect the binding and activation of a water substrate as well as the proton coupled electron transfer and the redox properties of the cluster.[5] More broadly, metals that are typically redox inactive at biologically relevant potentials affect the chemistry of a variety of redox processes,[6] particularly involving transition metals, including dioxygen and peroxide activation,[7] O- and H atom transfer,[8] alkane oxidation,[9] electron transfer rates, and reduction potentials.[10] Crystallographic characterization of metal-oxo species involved in this chemistry that display both the redox inactive and active metals is rare.[7a,10d] Toward addressing the role of Ca^{2+} in PSII, synthetic models have been targeted,[11] with small clusters displaying the biologically relevant CaMn$_3$O$_4$ cubane motif being recently reported.[12] To facilitate structure−function studies that interrogate the effect of redox inactive metals in clusters, we have developed synthetic protocols for heterometallic models of the biological system that allow for the incorporation of diverse metals

starting from trimetallic precursors and the generation of site-differentiated clusters.[13] Studies of structurally related MMn$_3$O$_4$, MMn$_3$O$_2$, MFe$_3$O(OH) clusters revealed a linear dependence of the reduction potential vs the pKa of the corresponding metal aqua ion as a measure of Lewis acidity.[13a,d,e] The significant slopes (70−100 mV/pKa unit) point to a role of the Lewis acid in tuning the cluster potential toward the appropriate level necessary for redox chemistry. Herein, we extend our synthetic, structural, and electrochemical studies to Mn cubanes displaying lanthanides, LnMn$_3$O$_4$, to evaluate how their systematic trends affect the properties of the clusters.

The lanthanides are an appealing choice in investigating systematic effects on the clusters' physical properties given the monotonic change in radius and chemical properties.[14] The preference of the lanthanides primarily for a single oxidation state simplifies the redox states available to the clusters.[14] Additionally, lanthanides have been used as substitutes for Ca^{2+} in biological systems because of the similarities in their ionic radii and high coordination numbers.[15]

The $[LnMn_3O_4]$ cubanes were targeted via a synthetic protocol previously employed for Zn^{2+}, Sc^{3+}, and Y^{3+}. More Lewis acidic metals can substitute for Ca^{2+} in the Mn$_3$CaO$_4$ cubane.[13d,f] The heteronuclear $[LnMn_3O_4]$ complexes were
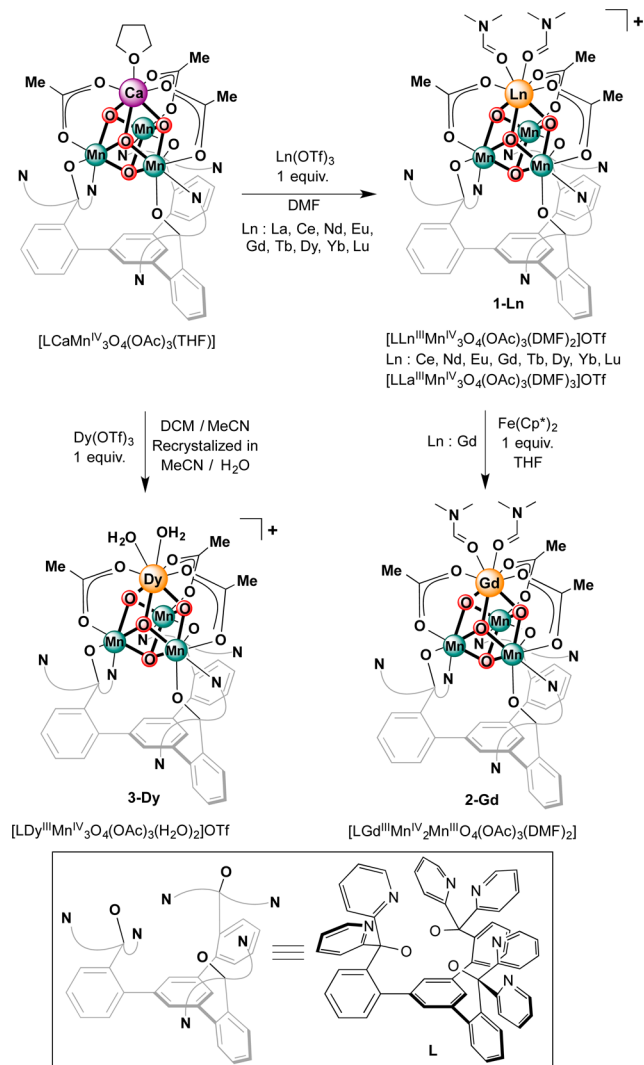
synthesized by treatment of LCaMn$_3$O$_4$(OAc)$_3$(THF) with Ln(OTf)$_3$ (Ln = La^{3+}, Ce^{3+}, Nd^{3+}, Eu^{3+}, Gd^{3+}, Tb^{3+}, Dy^{3+}, Yb^{3+}, Lu^{3+}) in dimethylformamide (DMF) (Scheme 1). The more

Scheme 1. Synthesis of Lanthanide-Mn-Oxide Clusters

Lewis acidic lanthanide ions readily substitute Ca^{2+}, as supported by ESI-MS data indicating the incorporation of the respective lanthanide ion and loss of Ca^{2+}. The ^{1}H NMR spectra of the all resulting clusters are broad and paramagnetically shifted. Nevertheless, they show features similar to the starting material, in particular a broad peak upfield of −15 ppm (see the Supporting Information).

To confirm the formation of the cubane moiety, we performed single-crystal XRD studies for a subset of [LnMn$_3$O$_4$] complexes based on the size of the lanthanide. Clusters displaying large (La^{3+}), intermediate (Gd^{3+}), and small (Yb^{3+}) lanthanides were selected for structural characterization in order to provide insight into the coordination environment as a function of the apical ion size. Dark brown crystals were grown by slow vapor diffusion of Et$_2$O into a CH$_2$Cl$_2$/DMF (2:1 v/v) solution of the metal complexes, over the course of several days. [LYb^{III}Mn$^{IV}_3$O$_4$(OAc)$_3$(DMF$_3$)](OTf) (**1-Yb**) and [LGd^{III}Mn$^{IV}_3$O$_4$(OAc)$_3$(DMF$_3$)](OTf) (**1-Gd**) have very similar structures (see Figure 1), displaying eight-coordinate lanthanide ions: three bridging oxides, three bridging acetates,
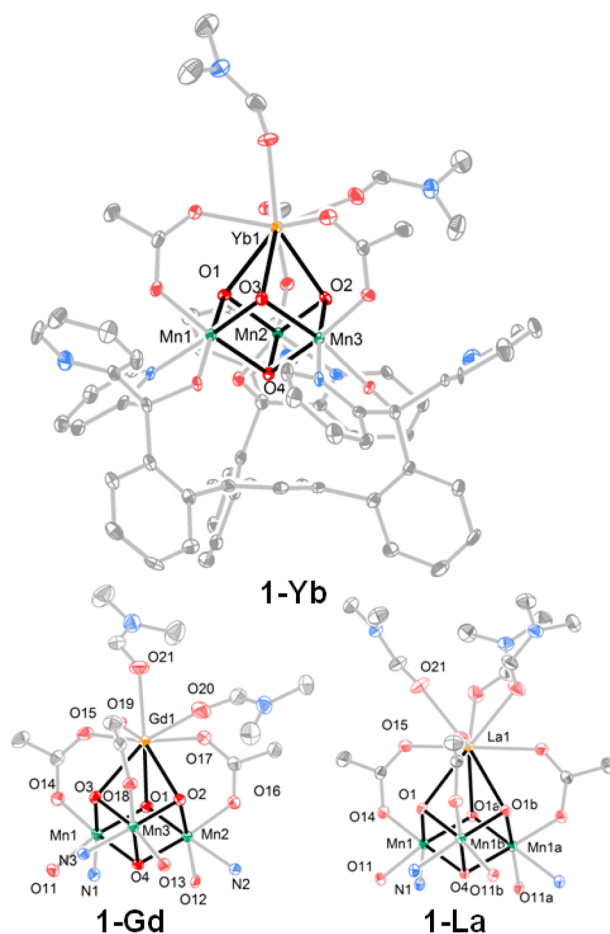

Figure 1. Solid-state structure of **1-Yb** and the cubane core structures of **1-Gd** and **1-La**. Outer sphere solvents and anions and hydrogen atoms are omitted for clarity.

and two DMF ligands. In contrast, the larger La^{3+} ion (**1-La**) accommodates a ninth ligand in an additional DMF molecule. Structural parameters (Figure 2), reflect the change in average Ln-oxido bond distances from 2.57 Å (La^{3+}) to 2.35 Å (Yb^{3+}) with the size of the lanthanide. Consequently, the average Ln-Mn distance decreases from 3.45 Å (La^{3+}) to 3.23 Å (Yb^{3+}).
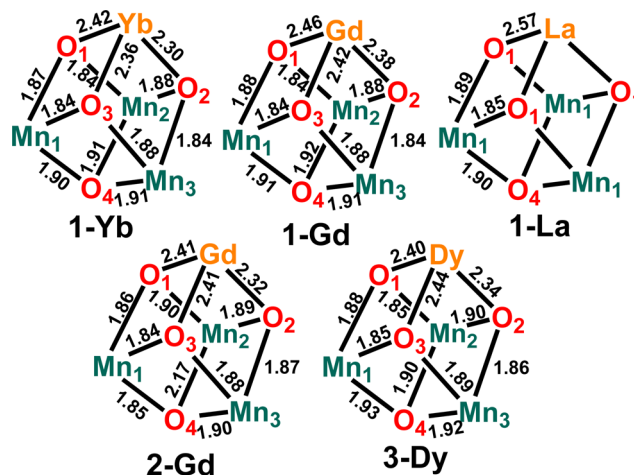

Figure 2. Metal-oxido distances of **1-Ln** (Ln = La, Gd, and Yb), **2-Gd**, and **3-Dy** in Å.

The Mn-oxido distances remain essentially the same, independent of the nature of Ln.

With a series of nine **1-Ln** complexes in hand, the effect of changing the nature of the lanthanide on the redox-properties of the clusters was studied by cyclic voltammetry (CV). The CVs of all complexes display a quasireversible wave assigned as the $[MMn^{IV}_3O_4]/[MMn^{IV}_2Mn^{III}O_4]$ couple (Figure 3 and
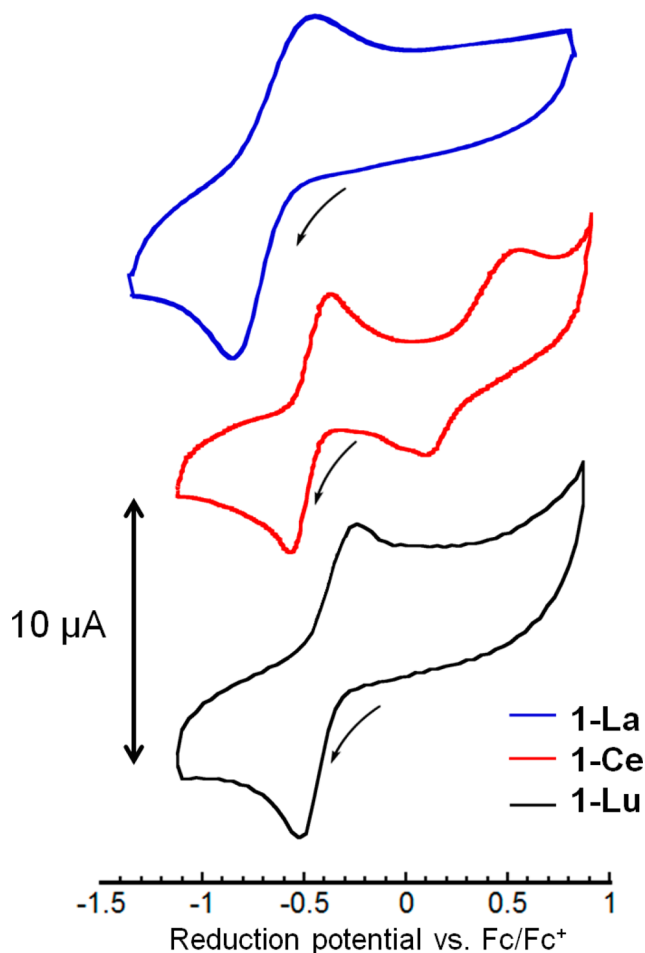

Figure 3. Cyclic voltammograms of **1-La**, **1-Ce**, and **1-Lu** in 0.1 M NBu_4PF_6 solution in DMA at a scan rate of 100 mV/s. Potentials are referenced to Fc/Fc$^+$.

Figures S14−19 in the Supporting Information). The reduction potentials vary within the range of −0.35 (**1-Lu**) to −0.49 V (**1-La**) vs the ferrocene/ferrocenium couple (Fc/Fc$^+$) (see Table S3 in the Supporting Information). Besides the quasi-reversible wave at −0.46 V assigned to $[MMn^{IV}_3O_4]/[MMn^{IV}_2Mn^{III}O_4]$, the CV of **1-Ce** exhibits an oxidation event at +0.62 V attributed to the oxidation from Ce^{III} to Ce^{IV}.[16] The two overlapping features for the reduction process at that potential suggest further chemical events following this oxidation.

A plot of the $E_{1/2}$ values vs the pKa values of the lanthanide aqua ions, M(aqua)$^{3+}$, revealed a linear correlation (Figure 4).[17a] We have previously reported similar linear $E_{1/2}$ vs pKa correlations,[13a,d,e] but with wider variation in the Lewis acidity of the metal and, therefore, over a wider range of pKa and potential values. For the lanthanide series, the pKa variation is relatively narrow leading to a potential range of less than 150 mV. It is notable that even in this small range, the plot of redox potential vs pKa remains linear.[18] When plotted with previously
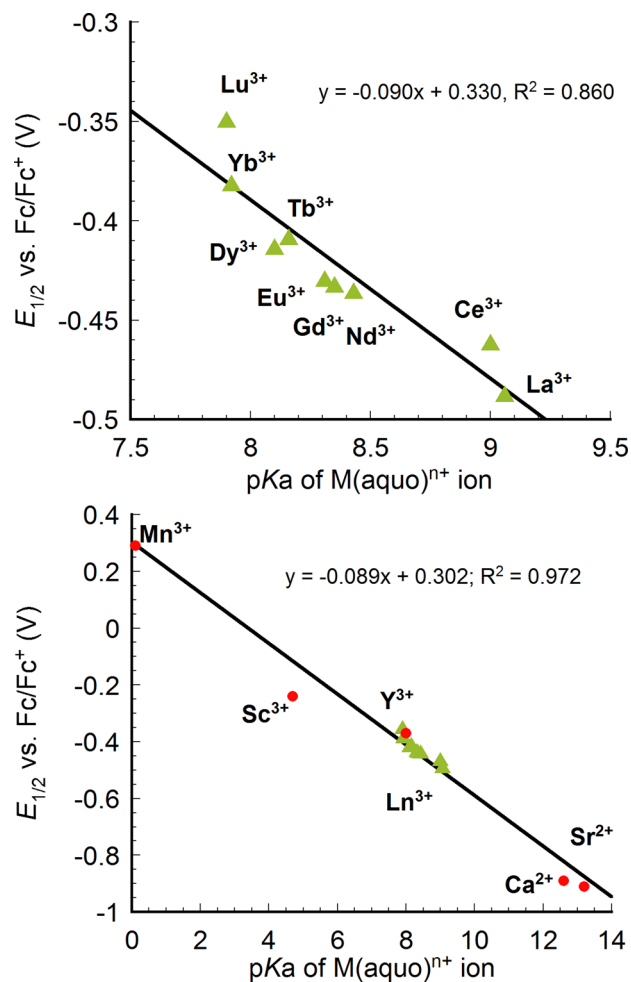

Figure 4. Plot of reduction potentials of $[LnMn_3O_4]$ (green triangle(top and bottom)) and previously reported $[MMn_3O_4]$ complexes (red circle(bottom)) vs pK$_a$ of the corresponding M(aqua)$^{n+}$ ion as a measure of Lewis acidity. Potentials were referenced to Fc/Fc$^+$.

reported cubanes, the lanthanide series fits well on the line (Figure 4).

With the expanded series of available M^{3+} cations in the composition of the $[MMn_3O_4]$ cubanes, the redox potentials were plotted against the radius of M, including Mn^{3+}, Sc^{3+}, Y^{3+}, and Ln^{3+} (Figure 5).[17b] Here as well, a linear correlation was observed between the potential and ionic radii of the rare earth ions. As expected, the reduction potential becomes more negative as the ionic radii increases and the Lewis acidity decreases. Mn^{III} is well-removed from the line generated by the rare earth ions. This is likely a consequence of the different bonding character of these metals.[14] The rare earth elements display primarily ionic interactions, therefore, the variation in radius is directly correlated to Lewis acidity giving linear dependence of redox potential vs both pKa and radius. Mn^{III} is more covalent, and the change in radius does not track directly with its Lewis acidity. Therefore, the pKa of metal aquo complexes is favored as a measure of Lewis acidity as it incorporates a composite of effects including changes in the nature of bonding, radius, charge, and number of ligands.

Access to the above heterometallic clusters allows for further synthetic elaboration. To confirm the nature of the reduced species evidenced in the CV studies, we performed the
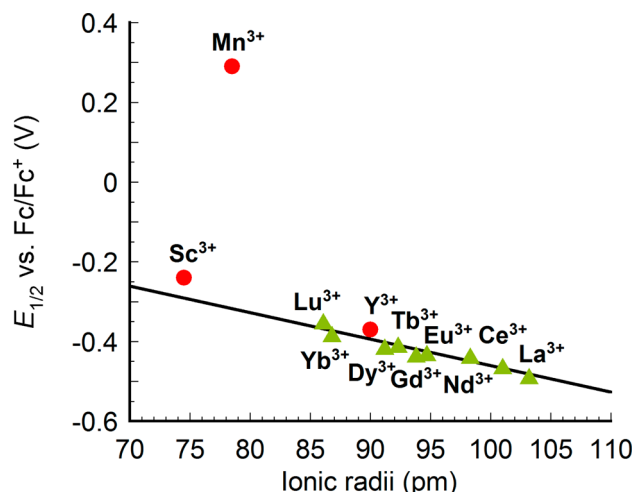
Figure 5. Plot of reduction potentials of $[Ln^{III}Mn_3O_4]$ complexes (green triangle) and other $[M^{III}Mn_3O_4]$ complexes (red circle) vs ionic radii of the corresponding $M(aqua)^{n+}$ ion.

chemical reduction of **1-Gd** with decamethylferrocene. The reduced species, **2-Gd**, was studied by XRD. Comparing the solid state structures of **1-Gd** and **2-Gd** (Figures 1, 6), the site
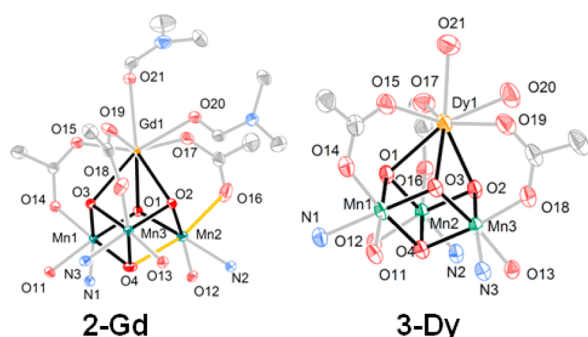

Figure 6. Solid-state structures of **2-Gd** and **3-Dy**. Only cubane core shown, for clarity. The elongated Mn−O bonds in **2-Gd** are highlighted in orange.

of reduction is localized at Mn2 in **2-Gd**. The Mn^{III} center displays an elongation of the O4−Mn2−O16 axis due to population of a σ-antibonding orbital. The bond lengths along this axis (2.169(1) Å for Mn2−O4; 2.163(1) Å for Mn2−O16) are over 0.2 Å longer in comparison to the Mn−oxide bonds in **1-Gd** (1.916(2)−1.941(2) Å) as well as the Mn−oxide bonds of Mn1 and Mn3 in **2-Gd** (1.8473(9)−1.897(1) Å), which are assigned to Mn^{IV} centers. **2-Gd** represents a rare example of mixed valent heterometallic cluster structurally related to the OEC. An analogous cluster, $[ScMn^{IV}_2Mn^{III}O_4]$, displays a similar localization of charge at Mn centers.[13d] Oxidation chemistry was also investigated with **1-Ce**, by treatment with tris(p-tolyl)ammoniumyl triflate. A new species was generated (^{1}H NMR spectroscopy) assigned as the $[Ce^{IV}Mn^{IV}_3]$ cluster, although attempts to grow single crystals for structural characterization have been unsuccessful to date.

In addition to redox chemistry, ligand substitution was investigated with these clusters. In particular, Ca^{2+}-coordinated water ligands have been proposed to be involved in O−O bond formation and are observed in the crystal structure of PSII.[2b,5b,c] In this context investigating the coordination of water and other ligands to cubane clusters is of interest. NMR

experiments of **1-Gd** in the presence of excess DMF show only one set of peaks for the ligand indicating fast exchange between bound and free DMF, that could not be frozen at low temperature (−40 °C) (see Figure S12 in the Supporting Information). Targeting water coordination, the Ca^{2+}/Dy^{3+} substitution was performed in the absence of DMF. Crystallization in the presence of water afforded **3-Dy** (Scheme 1) displaying water molecules bound to Dy^{3+} (Figure 6). The coordination of two water molecules to the lanthanide ion is reminiscent of the structure of the OEC.[2b,13a] In addition to modeling substrate binding as in the biological system, the isolation of **3-Dy** also highlights the stability of the reported clusters in the presence of water, important for further mechanistic studies.

In summary, mixed metal oxide clusters of Mn and Ln displaying the cubane structural motif relevant to the OEC have been synthesized and studied. Nine complexes spanning the lanthanide series have been prepared in the redox state $[LnMn^{IV}_3O_4]$ via Ca^{2+} substitution with Ln^{3+} from a $[CaMn^{IV}_3O_4]$ precursor. A linear dependence was observed between the reduction potentials of these complexes and the pKa of the metal aquo, $[Ln(H_2O)_n]^{3+}$, or the radius of Ln^{3+} indicating that the Lewis acidity of the nonmanganese ion tunes the potential of the cluster. A rare one-electron-reduced mixed valent cubane, $[GdMn^{IV}_2Mn^{III}O_4]$, was characterized by XRD and showed charge localization displayed by an axial distortion due to population of a σ-antibonding orbital. Reminiscent of binding of water molecules to Ca^{2+} in the biological system, a cluster displaying two water ligands bound to Dy^{3+} was structurally characterized and highlights the stability of the present models and their suitability for further mechanistic studies related to PSII.

■ EXPERIMENTAL SECTION

General Considerations. Unless otherwise specified, all compounds were manipulated using a glovebox or standard Schlenk line techniques with an N$_2$ atmosphere. Anhydrous tetrahydrofuran (THF) was purchased from Aldrich in 18 L Pure-Pac containers. Anhydrous acetonitrile, benzene, dichloromethane, diethyl ether, and THF were purified by sparging with nitrogen for 15 min and then passing under nitrogen pressure through a column of activated A2 alumina (Zapp's). Anhydrous N,N-dimethylformamide (DMF) was purchased from Aldrich and stored over molecular sieves. CD$_2$Cl$_2$ was purchased from Cambridge Isotope Laboratories, dried over calcium hydride, then degassed by three freeze−pump−thaw cycles and vacuum-transferred prior to use. ^{1}H NMR spectra were recorded on a Varian 300 MHz instrument, with shifts reported relative to the residual solvent peak. ^{19}F NMR spectra were recorded on a Varian 300 MHz instrument, with shifts reported relative to the internal lock signal. Elemental analyses were performed by Robertson Microlit Laboratories, NJ. All commercial chemicals were used as received. Ln(OTf)$_3$ (Ln= La, Ce, Nd, Eu, Gd, Tb, Dy, Yb, Lu) were purchased from Strem. LMn$_3$CaO$_4$(OAc)$_3$(THF) was prepared according to the previously published procedure.[13f]

Synthesis of [LLaMn$_3$O$_4$(OAc)$_3$(DMF)$_3$](OTf) (1-La) and [LLnMn$_3$O$_4$(OAc)$_3$(DMF)$_2$](OTf) (Ln: Ce (1-Ce), Nd (1-Nd), Eu (1-Eu), Gd (1-Gd), Tb (1-Tb), Dy (1-Dy), Yb (1-Yb), Lu (1-Lu)). A solution of Ln(OTf)$_3$ (0.02 mmol) in DMF (2 mL) was added to LMn$_3$CaO$_4$(OAc)$_3$(THF) (0.0274g, 0.02 mmol) solution in DMF (1 mL). The dark brown solution was stirred for an hour and then diethyl ether was added to precipitate the red-brown product. The precipitate was collected over Celite and extracted with CH$_2$Cl$_2$. The dark brown CH$_2$Cl$_2$ filtrate was concentrated in vacuo and crystallized from CH$_2$Cl$_2$/DMF/diethyl ether (1:1:5, v/v) to yield the product as red-brown crystals.

1-La: ^{1}H NMR (CD$_2$Cl$_2$, 300 MHz): δ 16.6, 11.7, 11.1, 9.2, 7.9, 5.9, 5.3, 4.7, 3.0 1.2, 0.9, −18.5 ppm. ^{19}F NMR (CD$_2$Cl$_2$, 282 MHz): δ −76.2 ppm. Yield: 88%. Anal. Calcd For C$_{72}$H$_{68}$F$_3$LaMn$_3$N$_9$O$_{19}$S: C, 49.24; H, 3.90; N, 7.18. Found: C, 49.52; H, 3.88; N, 7.03.

1-Nd: ^{1}H NMR (CD$_2$Cl$_2$, 300 MHz): δ 16.3, 11.5, 10.5, 10.1, 9.5, 5.6, 5.3, 3.5, 1.3, 0.9, −19.0 ppm. ^{19}F NMR (CD$_2$Cl$_2$, 282 MHz): δ −77.1 ppm. Yield: 86% Anal. Calcd For C$_{70}$H$_{62}$F$_3$Mn$_3$N$_8$NdO$_{18}$S: C, 49.42; H, 3.67; N, 6.59. Found: C, 49.37; H, 3.80; N, 5.61.

1-Ce: ^{1}H NMR (CD$_2$Cl$_2$, 300 MHz): δ 18.3, 13.5, 13.1, 12.5, 11.5, 10.8, 7.3, 7.2, 3.3, 2.1, −17.0 ppm. ^{19}F NMR (CD$_2$Cl$_2$, 282 MHz): δ −76.4 ppm. Yield: 41%. Anal. Calcd For C$_{73}$H$_{68}$CeCl$_6$F$_3$Mn$_3$N$_8$O$_{18}$S: C, 44.92; H, 3.51; N, 5.74. Found: C, 44.83; H, 3.27; N, 6.12.

1-Eu: ^{1}H NMR (CD$_2$Cl$_2$, 300 MHz): δ 15.9, 12.0, 11.7, 9.0, 6.8, 6.4, 5.4, 4.9, 4.0, 3.5, 2.7, 2.5, 1.7, 1.2, 1.0, 0.90, −20.46 ppm. ^{19}F NMR (CD$_2$Cl$_2$, 282 MHz): δ −74.6 ppm. Yield: 95%. Anal. Calcd For C$_{70}$H$_{62}$EuF$_3$Mn$_3$N$_8$O$_{18}$S: C, 49.19; H, 3.66; N, 6.56. Found: C, 49.24; H, 3.72; N, 6.59.

1-Gd: ^{1}H NMR (CD$_2$Cl$_2$, 300 MHz): δ 16.8, 11.9, 9.3, 6.0, 5.3, 3.0, 1.3, 1.2, −20.8 ppm. ^{19}F NMR (CD$_2$Cl$_2$, 282 MHz): δ −77.2 ppm. Anal. Yield: 98%. Calcd For C$_{70}$H$_{62}$F$_3$GdMn$_3$N$_8$O$_{18}$S: C, 49.04; H, 3.65; N, 6.54. Found: C, 49.13; H, 3.71; N, 6.64.

1-Tb: ^{1}H NMR (CD$_2$Cl$_2$, 300 MHz): δ 27.1, 17.9, 16.7, 15.3, 12.9, 9.0, 7.5, 6.7, 5.5, 3.6, 1.8, 1.4, 0.0, −1.4, −17.7 ppm. ^{19}F NMR (CD$_2$Cl$_2$, 282 MHz): δ −81.2 ppm. Yield: 93%. Anal. Calcd For C$_{70}$H$_{62}$F$_3$Mn$_3$N$_8$O$_{18}$STb: C, 48.99; H, 3.64; N, 6.53. Found: C, 49.13; H, 3.58; N, 6.46.

1-Dy: ^{1}H NMR (CD$_2$Cl$_2$, 300 MHz): δ 36.1, 21.1, 18.2, 17.3, 15.7, 10.4, 8.0, 5.3, 4.6, 3.4, 2.0, 1.3, −4.0, −16.6−42.0 ppm. ^{19}F NMR (CD$_2$Cl$_2$, 282 MHz): δ −90.4 ppm. Yield: 92%. Anal. Calcd For C$_{70}$H$_{62}$DyF$_3$Mn$_3$N$_8$O$_{18}$S: C, 48.89; H, 3.63; N, 6.52. Found: C, 48.84; H, 3.70; N, 6.62.

1-Yb: ^{1}H NMR (CD$_2$Cl$_2$, 300 MHz): δ 16.2, 14.5, 13.6, 9.3, 7.5, 5.6, 4.2, 3.7, 2.6, 1.7, 1.5, 1.2, −24.1 ppm. ^{19}F NMR (CD$_2$Cl$_2$, 282 MHz): δ −78.4 ppm. Yield: 80%. Anal. Calcd For C$_{73}$H$_{69}$F$_3$Mn$_3$N$_9$O$_{19}$SYb: C, 48.62; H, 3.86; N, 6.99. Found: C, 48.49; H, 3.66; N, 7.31.

1-Lu: ^{1}H NMR (CD$_2$Cl$_2$, 300 MHz): δ 14.2, 11.4, 11.0, 8.8, 7.3, 6.7, 5.5, 4.7, 3.7, 2.8, 2.2, 0.5, −23.4 ppm. ^{19}F NMR (CD$_2$Cl$_2$, 282 MHz): δ −76.7 ppm. Yield: 42% Anal. Calcd For C$_{70}$H$_{62}$F$_3$LuMn$_3$N$_8$O$_{18}$S: C, 48.54; H, 3.61; N, 6.47. Found: C, 48.27; H, 3.86; N, 6.64.

Synthesis of 2-Gd. A solution of **1-Gd** (0.037 g, 0.02 mmol) in THF (2 mL) was added to a decamethylferrocene (0.007 g, 0.02 mmol) solution in THF (2 mL). The dark brown solution was stirred overnight. A dark-brown precipitate was collected on a fritted glass funnel and washed with MeCN (4 mL) to remove the remaining [Cp*$_2$Fe]$^+$. The filter cake was washed with DCM, then dissolved in benzene/THF (1:1, v/v) and concentrated in vacuo. The resulting dark brown residue was recrystallized from DMF/benzene/diethyl ether (1:3:10, v/v) to yield the product as dark brown crystals. ^{1}H NMR (C$_6$D$_6$, 300 MHz): δ 7.1, 3.5, 3.2,1.6, 1.4, 1.1 ppm. Yield: 49%. Anal. Calcd for C$_{64}$H$_{50}$Cl$_2$GdMn$_3$N$_6$O$_{13}$: C, 51.11; H, 3.35; N, 5.59. Found: C, 50.92; H, 3.30; N, 5.81.

Synthesis of 3-Dy. Performed in air, a solution of Dy(OTf)$_3$ (0.02 mmol) in MeCN (1 mL) was added to [LMn$_3$CaO$_4$(OAc)$_3$(THF)] (0.0274g, 0.02 mmol) in DCM (2 mL). Dark brown solution was stirred magnetically for overnight until the solution became homogeneous. A single-solvent system was tried but the reaction could not be completed because Dy(OTf)$_3$ is poorly soluble in DCM and the CaMn$_3$ cubane is poorly soluble in MeCN. The solution was filtered by Celite and the product was concentrated in vacuo. The product was recrystallized from H$_2$O/MeCN/diethyl ether (1:10:30, v/v) to yield the product as red-brown crystals. ^{1}H NMR (CD$_2$Cl$_2$, 300 MHz): δ 80.9, 44.5, 22.6, 17.6, 14.3, 11.7, 8.3, 6.2, 5.3, 2.0, 1.5, 1.1, 0.3, −18.5 ppm. Yield: 91%. Anal. Calcd for C$_{69}$H$_{63}$Cl$_4$DyF$_3$Mn$_3$N$_9$O$_{19}$S: C, 43.09; H, 3.30; N, 5.10. Found: C, 42.82; H, 2.90; N, 5.17.

Synthesis of [LMn$_3$CeO$_4$(OAc)$_3$(DMF)$_3$](OTf)$_2$. In glovebox, a solution of **1-Ce** (75 mg, 0.042 mmol) in DCM (5 mL) was added with a DCM (5 mL) solution of tris(p-tolyl)ammoniumyl triflate (29.4 mg, 0.047 mmol), which was synthesized following procedure in the literature.[19] Color of the solution turned from dark brown to dark

orange brown. Mixture was stirred magnetically for 10 min and dried in vacuo. Diethyl ether was added to wash the mixture until filtrate cake becoming colorless and solid was collected over Celite. The filter cake was dissolved in DCM (∼5 mL) and the mixture was filtered through Celite. The filtrate was concentrated in vacuo to yield crystalline dark brown product. ^{1}H NMR (CD$_2$Cl$_2$, 300 MHz): δ 11.8, 9.7, 6.0, 4.5, 3.2, 23.2 ppm. Yield: 95%. Anal. Calcd For C$_{76}$H$_{73}$CeCl$_4$F$_6$Mn$_3$N$_9$O$_{22}$S$_2$: C, 43.69; H, 3.52; N, 6.03. Found: C, 43.97; H, 3.19; N, 6.30.

■ ASSOCIATED CONTENT

Ⓢ Supporting Information

Experimental procedures and spectroscopic characterization, and crystallographic (CIF) data. This material is available free of charge via the Internet at http://pubs.acs.org.

■ AUTHOR INFORMATION

Corresponding Author

*E-mail: agapie@caltech.edu.

Notes

The authors declare no competing financial interest.

■ REFERENCES

(1) (a) McEvoy, J. P.; Brudvig, G. W. *Chem. Rev.* **2006**, *106*, 4455. (b) Wydrzynski, T. J.; Satoh, K. *Photosystem II: The Light-Driven Water: Plastoquinone Oxidoreductase*; Springer: Dordrecht, The Netherlands, 2005; Vol. 22. (c) Yano, J.; Yachandra, V. *Chem. Rev.* **2014**, *114*, 4175.

(2) (a) Ferreira, K. N.; Iverson, T. M.; Maghlaoui, K.; Barber, J.; Iwata, S. *Science* **2004**, *303*, 1831. (b) Umena, Y.; Kawakami, K.; Shen, J. R.; Kamiya, N. *Nature* **2011**, *473*, 55.

(3) (a) Kok, B.; Forbush, B.; Mcgloin, M. *Photochem. Photobiol.* **1970**, *11*, 457. (b) Joliot, P.; Barbieri, G.; Chabaud, R. *Photochem. Photobiol.* **1969**, *10*, 309.

(4) Yocum, C. F. *Coord. Chem. Rev.* **2008**, *252*, 296.

(5) (a) Yachandra, V. K.; Sauer, K.; Klein, M. P. *Chem. Rev.* **1996**, *96*, 2927. (b) Pecoraro, V. L.; Baldwin, M. J.; Caudle, M. T.; Hsieh, W. Y.; Law, N. A. *Pure Appl. Chem.* **1998**, *70*, 925. (c) Vrettos, J. S.; Stone, D. A.; Brudvig, G. W. *Biochemistry* **2001**, *40*, 7937. (d) Riggs-Gelasco, P. J.; Mei, R.; Ghanotakis, D. F.; Yocum, C. F.; Penner-Hahn, J. E. *J. Am. Chem. Soc.* **1996**, *118*, 2400. (e) Lohmiller, T.; Cox, N.; Su, J.-H.; Messinger, J.; Lubitz, W. *J. Biol. Chem.* **2012**, *287*, 24721.

(6) (a) Fukuzumi, S.; Ohkubo, K. *Coord. Chem. Rev.* **2010**, *254*, 372. (b) Fukuzumi, S. In *Prog. Inorg. Chem.*; John Wiley & Sons: New York, 2009; Vol. *56*, p 49.

(7) (a) Park, Y. J.; Ziller, J. W.; Borovik, A. S. *J. Am. Chem. Soc.* **2011**, *133*, 9258. (b) Park, Y. J.; Cook, S. A.; Sickerman, N. S.; Sano, Y.; Ziller, J. W.; Borovik, A. S. *Chem. Sci.* **2013**, *4*, 717. (c) Li, F.; Van Heuvelen, K. M.; Meier, K. K.; Muenck, E.; Que, L., Jr. *J. Am. Chem. Soc.* **2013**, *135*, 10198. (d) Lee, Y. M.; Bang, S.; Kim, Y. M.; Cho, J.; Hong, S.; Nomura, T.; Ogura, T.; Troeppner, O.; Ivanovic-Burmazovic, I.; Sarangi, R.; Fukuzumi, S.; Nam, W. *Chem. Sci.* **2013**, *4*, 3917.

(8) (a) Leeladee, P.; Baglia, R. A.; Prokop, K. A.; Latifi, R.; de Visser, S. P.; Goldberg, D. P. *J. Am. Chem. Soc.* **2012**, *134*, 10397. (b) Dong,

L.; Wang, Y. J.; Lv, Y. Z.; Chen, Z. Q.; Mei, F. M.; Xiong, H.; Yin, G. C. *Inorg. Chem.* **2013**, *52*, 5418.

(9) Yiu, S. M.; Man, W. L.; Lau, T. C. *J. Am. Chem. Soc.* **2008**, *130*, 10821.

(10) (a) Morimoto, Y.; Kotani, H.; Park, J.; Lee, Y. M.; Nam, W.; Fukuzumi, S. *J. Am. Chem. Soc.* **2011**, *133*, 403. (b) Horwitz, C. P.; Ciringh, Y.; Weintraub, S. T. *Inorg. Chim. Acta* **1999**, *294*, 133. (c) Horwitz, C. P.; Ciringh, Y. *Inorg. Chim. Acta* **1994**, *225*, 191. (d) Fukuzumi, S.; Morimoto, Y.; Kotani, H.; Naumov, P.; Lee, Y. M.; Nam, W. *Nat. Chem.* **2010**, *2*, 756. (e) Chen, J.; Lee, Y. M.; Davis, K. M.; Wu, X.; Seo, M. S.; Cho, K. B.; Yoon, H.; Park, Y. J.; Fukuzumi, S.; Pushkar, Y. N.; Nam, W. *J. Am. Chem. Soc.* **2013**, *135*, 6388. (f) Yoon, H.; Lee, Y.-M.; Wu, X.; Cho, K.-B.; Sarangi, R.; Nam, W.; Fukuzumi, S. *J. Am. Chem. Soc.* **2013**, *135*, 9186. (g) Fukuzumi, S. *Coord. Chem. Rev.* **2013**, *257*, 1564. (h) Nam, W.; Lee, Y. M.; Fukuzumi, S. *Acc. Chem. Res.* **2014**, *47*, 1146.

(11) Tsui, E. Y.; Kanady, J. S.; Agapie, T. *Inorg. Chem.* **2013**, *52*, 13833.

(12) (a) Kanady, J. S.; Tsui, E. Y.; Day, M. W.; Agapie, T. *Science* **2011**, *333*, 733. (b) Mukherjee, S.; Stull, J. A.; Yano, J.; Stamatatos, T. C.; Pringouri, K.; Stich, T. A.; Abboud, K. A.; Britt, R. D.; Yachandra, V. K.; Christou, G. *Proc. Natl. Acad. Sci. U.S.A.* **2012**, *109*, 2257. (c) Kanady, J. S.; Lin, P.-H.; Carsch, K. M.; Nielsen, R. J.; Takase, M. K.; Goddard, W. A., III; Agapie, T. *J. Am. Chem. Soc.* **2014**, *136*, 14373.

(13) (a) Tsui, E. Y.; Tran, R.; Yano, J.; Agapie, T. *Nat. Chem.* **2013**, *5*, 293. (b) Tsui, E. Y.; Kanady, J. S.; Day, M. W.; Agapie, T. *Chem. Commun.* **2011**, *47*, 4189. (c) Tsui, E. Y.; Day, M. W.; Agapie, T. *Angew. Chem., Int. Ed.* **2011**, *50*, 1668. (d) Tsui, E. Y.; Agapie, T. *Proc. Natl. Acad. Sci. U.S.A.* **2013**, *110*, 10084. (e) Herbert, D. E.; Lionetti, D.; Rittle, J.; Agapie, T. *J. Am. Chem. Soc.* **2013**, *135*, 19075. (f) Kanady, J. S.; Mendoza-Cortes, J. L.; Tsui, E. Y.; Nielsen, R. J.; Goddard, W. A.; Agapie, T. *J. Am. Chem. Soc.* **2013**, *135*, 1073. (g) Kanady, J. S.; Tran, R.; Stull, J. A.; Lu, L.; Stich, T. A.; Day, M. W.; Yano, J.; Britt, R. D.; Agapie, T. *Chem. Sci.* **2013**, *4*, 3986.

(14) Cotton, S. *Lanthanide and Actinide Chemistry*; John Wiley & Sons: Chichester, U.K., 2006.

(15) (a) Bakou, A.; Buser, C.; Dandulakis, G.; Brudvig, G.; Ghanotakis, D. F. *Biochim. Biophys. Acta* **1992**, *1099*, 131. (b) Bakou, A.; Ghanotakis, D. F. *Biochim. Biophys. Acta* **1993**, *1141*, 303. (c) Lee, C. I.; Lakshmi, K. V.; Brudvig, G. W. *Biochemistry* **2007**, *46*, 3211.

(16) Piro, N. A.; Robinson, J. R.; Walsh, P. J.; Schelter, E. J. *Coord. Chem. Rev.* **2014**, *260*, 21.

(17) (a) Perrin, D. D. *Ionisation Constants of Inorganic Acids and Bases in Aqueous Solution*; Pergamon: Oxford, U.K., 1982. Values of pKa reported under the same conditions (titration of 0.004−0.009 M Ln(ClO$_4$)$_3$ with 0.02 M Ba(OH)$_2$; I = 0.3, NaClO$_4$) were used for all ions except Ce^{III}. (b) *Acta Cryst.* **1976**, *A32*, 751

(18) One of the referees pointed out that the slope of the line in Figure 4 is close to unity if plotted on the same energy scale. We do not have an explanation for this behavior at this time.

(19) Barton, D. H. R.; Haynes, R. K.; Leclerc, G.; Magnus, P. D.; Menzies, I. D. *J. Chem. Soc., Perkin Trans.* **1975**, *1*, 2055.